

Kinetics of Peptide Binding to the Class II MHC Protein I–E^{k†}Peter M. Kasson,[‡] Joshua D. Rabinowitz,[‡] Lutz Schmitt,^{‡,§} Mark M. Davis,^{||} and Harden M. McConnell^{*,‡}*Department of Chemistry, Stanford University, Stanford, California 94305, and Howard Hughes Medical Institute, Stanford University Medical School, Stanford, California 94305**Received September 14, 1999*

ABSTRACT: Class II MHC glycoproteins bind short (7–25 amino acid) peptides in an extended type II polyproline-like conformation and present them for immune recognition. Because empty MHC is unstable, measurement of the rate of the second-order reaction between peptide and MHC is challenging. In this report, we use dissociation of a pre-bound peptide to generate the active, peptide-receptive form of the empty class II MHC molecule I–E^k. This allows us to measure directly the rate of reaction between active, empty I–E^k and a set of peptides that vary in structure. We find that all peptides studied, despite having highly variable dissociation rates, bind with similar association rate constants. Thus, the rate-limiting step in peptide binding is minimally sensitive to peptide side-chain structure. An interesting complication to this simple model is that a single peptide can sometimes bind to I–E^k in two kinetically distinguishable conformations, with the stable peptide–MHC complex isomer forming much more slowly than the less-stable one. This demonstrates that an additional free-energy barrier limits the formation of certain specific MHC–peptide complex conformations.

Class II MHC¹ are heterodimeric membrane glycoproteins expressed on the surface of antigen presenting cells of the immune system. Class II MHC are peptide receptors, binding a diverse array of peptides of approximately 7–25 amino acids in length and presenting them to CD4⁺ T lymphocytes. Recognition of specific peptide–MHC complexes by T cells is a key step in the generation of an immune response.

The process of peptide binding to MHC involves the peptide changing from an unstructured solution form to a type II polyproline helix-like extended conformation held in a defined backbone registry within the binding groove of the MHC molecule (see Figure 1) (1–5). Understanding peptide binding to MHC is of general interest because it is potentially useful for the design of vaccines, for understanding the roots of autoimmune disease, and also because the dynamics of the binding process likely resemble some steps of protein-folding reactions.

[†] P.M.K. was supported by Stanford University President's Scholar and Bing Fellowships and by the Biophysics Program. J. R. was supported by the Medical Scientist Training Program, and L. S. by the Deutsche Forschungsgemeinschaft. This research was funded by the Howard Hughes Medical Institute (M. M. D.) and the National Institute of Health (H. M. M., Grant 2R01 AI13587-24).

^{*} To whom correspondence should be addressed. Telephone: (650) 723-4571. Fax: (650) 723-4943. E-mail: harden@leland.stanford.edu.

[‡] Department of Chemistry.

[§] Current address: Institut fuer Physiologische Chemie, Philipps-Universitaet Marburg, 35033 Marburg, Germany.

^{||} Howard Hughes Medical School.

¹ Abbreviations: MHC, major histocompatibility complex; Ii, invariant chain; Hb, hemoglobin; HPLC, high-performance liquid chromatography; HPSEC, high-performance size-exclusion chromatography; PBS, phosphate-buffered saline (150 mM sodium chloride, 10 mM sodium phosphate, 0.02% sodium azide); PBS-citrate, PBS + 100 mM sodium citrate; PCC, pigeon cytochrome *c*. Single-letter abbreviations for amino acids used in this paper are as follows: A, alanine; D, aspartate; E, glutamate; F, phenylalanine; G, glycine; I, isoleucine; K, lysine; L, leucine; M, methionine; N, asparagine; P, proline; Q, glutamine; R, arginine; T, threonine; V, valine; Y, tryptophan. The nonnatural amino acid ornithine is abbreviated Or. The commonly studied peptide moth cytochrome *c* 95–103 is identical to PCC 95–103 A103K.

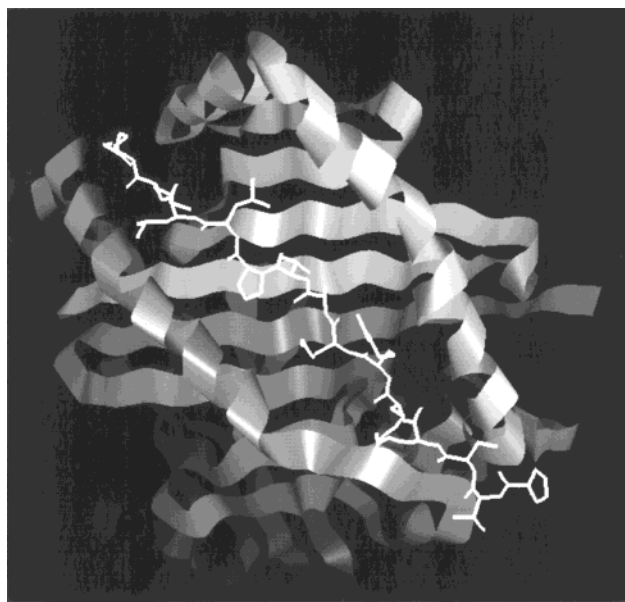


FIGURE 1: Invariant chain peptide bound to I–E^k. The peptide (Ii 86–99), shown in line form, is bound in an extended conformation, similar to a type II polyproline helix. The binding groove of the MHC heterodimer, shown in ribbon form, consists of a beta sheet floor and two alpha helical walls. One or both ends of the peptide may extend beyond the binding groove, which can hold up to nine amino acids. These nine positions are designated p1 through p9. In I–E^k, p1 and p9 have been identified as particularly important in determining complex stability (27, 34, 35). The model of I–E^k shown here was generated based on a crystal structure of a I–E^k by Fremont et al. (5) and using the software package Look (Molecular Applications Group).

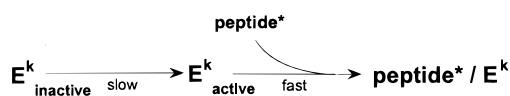
Early kinetic studies of peptide–MHC interactions revealed that many different peptides bind with moderate or high stability to any given MHC protein, with half-times of minutes to months for peptide dissociation. In addition, they found that peptide binding to MHC appeared to be very slow, with association rate constants of only 1–100 M⁻¹ s⁻¹, at

least 7 orders of magnitude below the diffusion limit (6–9). In attempting to understand the rate-limiting step in the process of peptide binding, two significant discoveries were made.

First, it was found that a single peptide may bind to a single MHC protein to form two isomeric complexes, identical in covalent composition but differing in stability (10–17). On the basis of the discovery of these isomers, it has been hypothesized that the short-lived complex might be a kinetic intermediate in the formation of the long-lived complex and that slow interconversion of the complexes is responsible for the slow apparent association rate of peptide to MHC (10). Further work has confirmed the presence of peptide–MHC complex isomers using NMR spectroscopy and demonstrated the ability of the different isomers to trigger distinct T cell responses (18, 19).

Recently, however, it was demonstrated that it is the presence of distinct isomers of empty (i.e., devoid of peptide) MHC (Scheme 1), not peptide–MHC complexes, that largely

Scheme 1

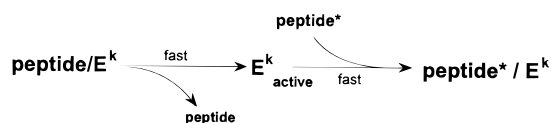


explains the slow apparent association rate of peptide to MHC (20–22). One isomer of empty MHC (inactive) does not bind peptide detectably. The other (active) binds peptide rapidly, approximately 1000-fold faster than previously estimated. The peptide-receptive, or active, form is released by dissociation of previously bound peptide and rapidly inactivates in the absence of added peptide. At equilibrium, the inactive form of empty MHC predominates, only slowly converting to the active form. This slow conversion of the inactive to the active form accounts for the slow binding of peptide to MHC observed in previous studies (Scheme 1).

Isomerization of empty MHC is regulated in antigen presenting cells by accessory molecules that localize the release of the peptide-receptive active isomer. Newly synthesized MHC heterodimers are assembled in the endoplasmic reticulum in conjunction with a molecule termed invariant chain (Ii) (23). In endosomes, Ii is proteolyzed, leaving only a short fragment of Ii (residues 81–104) bound to the MHC molecule. This fragment, known as class II-associated invariant chain-derived peptide (CLIP), dissociates, leaving the MHC molecule in the empty active state. CLIP dissociation in endosomes can be accelerated by a protein catalyzing peptide exchange (termed H2-M in mice and HLA-DM in humans) (24, 25).

To simulate the physiological antigen presentation pathway in a chemically defined manner, we used a water-soluble version of the MHC protein I–E^k that was uniformly loaded with CLIP and then allowed to dissociate for a brief period of time to generate a population of active I–E^k (Scheme 2).

Scheme 2



Labeled peptide was then added. The ensuing association reaction was not limited by the slow isomerization of inactive

I–E^k to active I–E^k and thus proceeded much more quickly than previously observed. Since CLIP dissociates very rapidly from I–E^k, the catalyst H2-M was not needed to speed dissociation. Using this method to measure the second-order association rate constant for peptide binding to active I–E^k, we find that 20 structurally varied peptides all bind to this MHC protein with similar association rate constants. This demonstrates that the free-energy barrier for peptide–MHC association is generally not very sensitive to peptide side-chain structure.

Since it is known that at least some of the peptides studied could bind to I–E^k to form multiple isomeric complexes, we also studied the stability of the complexes formed between each peptide and I–E^k after short and long association reactions. We find that most of the peptides studied form primarily one “kinetic” complex (that is, for any given peptide, most of the complexes formed can be characterized by a single dissociation rate constant). One peptide, however, binds with an association rate constant comparable to that of the other peptides to form unstable complexes, but only very slowly forms a highly stable complex. This suggests that formation of certain peptide–MHC complex isomers requires passing through a much higher transition barrier.

On the basis of these findings, we propose a model in which the transition states for peptide binding to MHC are registry-specific. Random selection of peptide-binding registries results in a variety of peptide–MHC complex intermediates, only a small fraction of which form stable complexes.

MATERIALS AND METHODS

Peptide Synthesis. All peptides studied were synthesized on an Applied Biosystems 431A peptide synthesizer, using standard Fmoc chemistry. N-terminal fluorescent labeling was performed by adding 5-(and 6-)carboxyfluorescein succinimidyl ester and 2% (vol/vol) *N,N*-diisopropylethylamine to the dry resin suspended in DMSO overnight in the dark. C-terminal labeling on PCC Ac95–103 A103K, PCC Ac96–103 A103K, and PCC Ac97–103 A103K was performed by synthesizing peptides with an additional amino acid on the C-terminus: *N*- α -Fmoc-*N*- ϵ -1-(4,4-dimethyl-2,6-dioxocyclohex-1-ylidene)ethyl-L-lysine. The –Dde protective group was removed using 2% hydrazine in DMF. A carboxyfluorescein label was attached to the ϵ -amino group using the same protocol as for N-terminal labeling. Peptides were cleaved from the resin and deprotected in 90% TFA, 5% thioanisole, and 5% ethanedithiol for 3 h, after which the peptide was precipitated using *tert*-butyl methyl ether, dried, dissolved in water/acetonitrile, then lyophilized. Purification and confirmation of identity were carried out by reverse-phase (RP18) HPLC using a water/0.1% TFA–acetonitrile/0.1% TFA gradient and high-resolution mass spectrometry. The sequences of all peptides used are given in Table 1.

MHC Preparation. Soluble I–E^k was produced in a glycosylphosphatidylinositol-linked form using Chinese hamster ovary cells and purified on an affinity column followed by high-performance size-exclusion chromatography (HPSEC) as similar to the method previously described (26). After purification, I–E^k was stored at 4 °C until preloading with peptide. I–E^k concentrations were determined using a microBCA protein assay or by UV absorption at 280 nm using a molar extinction coefficient of $1.4 \times 10^5 \text{ M}^{-1} \text{ cm}^{-1}$.

Table 1: Peptides Studied and the Kinetics of Their Reaction with I-E^k at pH 5.3 and 37 °C

| Peptide: | Putative Binding Pocket ^a | Dissociation ^b | | Association ^c | |
|----------------------|--------------------------------------|---------------------------|------------------------|------------------------------------|-----------|
| | | 1 6 9 | t _{1/2} Group | Rate | Magnitude |
| | | | (minutes) | (M ⁻¹ s ⁻¹) | (nM) |
| Ii f85-99 | KPVSQMRMATPLLMR | | 3 a | 1.4·10 ⁵ | 2.3 |
| Ii f89-99 | QMRMATPLLMR | | 25 a | 2.7·10 ⁵ | 2.5 |
| Ii f85-99 M90L | KPSVQLRMATPLLMR | | 100 a | 3.0·10 ⁵ | 3.6 |
| Ii f85-99 M90LM98L | KPSVQLRMATPLLRL | | 50 a | 4.0·10 ⁵ | 3.5 |
| Ii 85-99 P95E | KPSVQMRMATELLMR | | 7.5 a | 3.8·10 ⁵ | 1.7 |
| PCC f95-103 A103K | IAYLKQATK | | >10000 c | 1.5·10 ⁵ | 3.0 |
| PCC Ac95-103fK A103K | IAYLKQATK | | >10000 c | 1.7·10 ⁵ | 2.0 |
| PCC Ac96-103fK A103K | AYLKQATK | | 13 a | 6.9·10 ⁴ | 2.8 |
| PCC Ac97-103fK A103K | YLKQATK | | 3 a | 1.6·10 ⁵ | 1.6 |
| PCC f95-102 | IAYLKQAT | | 6 a | 3.7·10 ⁴ | 3.8 |
| PCC f95-101 | IAYLKQA | | 2 a | 1.8·10 ⁵ | 2.5 |
| PCC-P | IAPLPQPPK | | 7 a | 8.3·10 ⁴ | 3.2 |
| PCC-G | IAGLGQGGK | | 3 a | 7.0·10 ⁴ | 3.7 |
| PCC f89-103 | AERADLIAYLKQATA | | 230 b | 4.0·10 ⁴ | 2.3 |
| PCC f89-104 | AERADLIAYLKQATAK | | 460 b | 6.1·10 ⁴ | 3.3 |
| PCC f89-103 A103K | AERADLIAYLKQATK | | >10000 c | 4.5·10 ⁴ | 3.5 |
| PCC f89-104 Q100A | AERADLIAYLKAATAK | | 330 b | 4.5·10 ⁴ | 4.8 |
| PCC f89-104 A103K | AERADLIAYLKQATKK | | >10000 c | 4.4·10 ⁴ | 4.2 |
| PCC f89-104 Q100OR | AERADLIAYLKQrATAK | | ** ** | 5.4·10 ⁴ | 3.0 |
| Hb | GKKVITAFNDGLK | | 2770 c | 2.0·10 ⁵ | 3.4 |

^a Putative P1 pocket anchor of each peptide was determined based on crystallographic and T cell simulation data (5, 27, 33, and J. R., unpublished data). ^b Peptides were grouped based on their dissociation characteristics: a, rapid monophasic dissociation, as exemplified in Figure 5A; b, moderately slow, approximately monophasic dissociation, as exemplified in Figure 5B; c, minimal dissociation within 24 h, as exemplified in Figure 5C. ^c Peptide association was measured as in Figure 2. Data indicating the amount of complex formed at varying peptide concentrations were used to generate a single-exponential curve $[p/M] = [p]/([p] + K)[M_0](1 - e^{-(p+K)k_{on}t})$ where k_{on} is the estimated association rate constant and $[M_0]$ is the saturation magnitude of binding. Two independent measurements of the rate and magnitude were performed for four peptides. The mean percent error (100% × S.D./mean) was 13% for the rate and 19% for the magnitude. Maximum percent errors were 36% and 28%, respectively. ^{b,c} Note that the equilibrium constants calculated from k_{on} and k_{off} do not take into account the inactivation reaction shown in Scheme 4. ** Biphasic dissociation, with the dissociation behavior highly dependent on the duration of the association reaction; see Figure 6.

To generate a uniformly loaded peptide–MHC complex that dissociates rapidly, I–E^k was prepared as described above and then incubated with >50-fold excess unlabeled peptide at 37 °C and pH 5.3 in PBS-citrate (PBS, 100 mM sodium citrate). After 36 h, the preloading mixture was transferred to 4 °C and stored until immediately prior to use, at which point the peptide/I–E^k complex was separated from free peptide on a 2 mL disposable Sephadex G50-SF size exclusion column blocked with 10 mg/mL bovine serum albumen and equilibrated in PBS pH 7.

Peptide–MHC Binding Kinetics. The general approach we took to measuring peptide–MHC binding kinetics was to measure the peptide concentration-dependence of complex formation using a brief, fixed incubation duration. I–E^k preloaded with either Ii 85–99 or PCC Ac96–103 A103K (dissociation $t_{1/2}$ from I–E^k of 3 min and 5 min, respectively) was incubated for five minutes at 37 °C and pH 5.3 in PBS-citrate or pH 7 in PBS to allow the preloading peptide to

dissociate, releasing active I–E^k. Then a defined concentration of fluorescently labeled peptide was added and allowed to react at 37 °C and pH 5.3 or pH 7 for three minutes, at which point the mixture was injected onto an HPSEC column with an in-line fluorescence detector. HPSEC was performed using either TosoHaas column G3000SW or column G3000SWxl (Montgomeryville, PA) at room temperature with a flow rate of 1 mL/min of PBS pH 7.0. Elution times for the peptide/I–E^k complex were 16 min for the G3000SW column and 9 min for the G3000SWxl column. Both columns gave similar results. Relative amounts of peptide–MHC complex were compared based on the peak height of the fluorescence signal. These values were then normalized to absolute concentrations by comparing the signal with a given peptide to the signal obtained with a saturating concentration (86 nM) Ii f85–99 M90L peptide and then comparing the area under the fluorescence time curve for Ii f85–99 M90L to the area under the curve for known concentrations of car-

boxyfluorescein standard. Effects on fluorescence quantum yield due to interactions between the protein and the fluorophore such as quenching were not explicitly considered and could fully or partially explain variations in the maximal apparent binding observed for different peptide–MHC complexes.

Calculation of Association Rate Constants. Second-order association rate constants for peptide binding to active I–E^k were calculated using two reaction schemes: a highly simplified one and a more complex one (Schemes 3 and 4, respectively, in Results). Given a number of assumptions (see below), Scheme 4 can be approximated by Scheme 3. The differential equations corresponding to Scheme 3 are:

$$\begin{aligned}\frac{d[M_a]}{dt} &= -k_{on}[p][M_a] + k_{off}[p/M] \\ \frac{d[p]}{dt} &= -k_{on}[p][M_a] + k_{off}[p/M] \\ \frac{d[p/M]}{dt} &= k_{on}[p][M_a] - k_{off}[p/M]\end{aligned}\quad \text{eq 1}$$

where $[M_a]$ is the concentration of active MHC, $[p]$ is the concentration of peptide, $[p/M]$ is the concentration of peptide–MHC complex, k_{on} is the association rate constant, and k_{off} is the dissociation rate constant. If the peptide is in large excess, then one can take the concentration of peptide to be essentially constant and thus consider the reaction to be pseudo-first order. In this scheme, there is a constant amount of MHC present, so $[M_a] + [p/M] = [M_0]$. One can then solve the differential equations analytically to give the following single-exponential equation for association:

$$[p/M] = \frac{[p]}{[p] + K} [M_0] (1 - e^{-(p+K)k_{off}t}) \quad \text{eq 2}$$

where $K = k_{off}/k_{on}$.

The experimental data were fit to this equation using Kaleidagraph (Synergy Software). The association time was 180 s. The curve fit parameters are $[M_0]$ and k_{on} .

The differential equations corresponding to Scheme 4 are:

$$\begin{aligned}\frac{d[Ii/M]}{dt} &= -k_{-1}[Ii/M] + k_1[M_a][Ii] \\ \frac{d[Ii]}{dt} &= k_{-1}[Ii/M] - k_1[M_a][Ii] \\ \frac{dM_a}{dt} &= k_{-1}[Ii/M] - k_1[M_a][Ii] - k_{ai}[M_a] + k_{ia}[M_i] - \\ &\quad k_{on}[p][M_a] + k_{off}[p/M] \\ \frac{d[M_i]}{dt} &= k_{ai}[M_a] - k_{ia}[M_i] \\ \frac{d[p]}{dt} &= -k_{on}[p][M_a] + k_{off}[p/M] \\ \frac{d[p/M]}{dt} &= k_{on}[p][M_a] - k_{off}[p/M]\end{aligned}\quad \text{eq 3}$$

where $[Ii]$ is the concentration of unlabeled Ii 85–99, $[Ii/M]$ is the concentration of Ii–MHC complex, $[M_i]$ is the concentration of inactive MHC, $[M_a]$ is the concentration of active MHC, $[p]$ is the concentration of labeled peptide,

$[p/M]$ is the concentration of labeled peptide–MHC complex, k_1 is the rate constant for Ii association to MHC, k_{-1} is the rate constant for dissociation of the Ii–MHC complex, k_{ai} is the rate constant for inactivation of active MHC, k_{ia} is the rate constant for reactivation of inactive MHC, k_{on} is the rate constant for association of labeled peptide to MHC, and k_{off} is the rate constant for dissociation of labeled peptide from MHC. For a given set of initial values and rate constants, these equations can be solved numerically. All rate constants except for k_1 and k_{on} can be determined independently. To determine k_1 , one can use experimental data for the association of Ii f85–99 to I–E^k and assume that the fluorescent label does not have a significant effect on the association rate, so $k_1 = k_{on}$. The desired value for k_{on} is one where, when the differential equations are solved numerically, a single-exponential curve fit for $[p/M]$ as a function of $[p]$ (as described above) most closely resembles the corresponding fit for the experimental data. A search of rate constant space was performed with the above condition as the search metric. To similarly determine the association rate constants of other peptides, the process can be repeated leaving k_1 fixed to the association rate constant just determined for Ii 85–99.

The assumptions required to derive Scheme 3 from Scheme 4 are that the four reactions included in Scheme 4 but not Scheme 3 do not significantly affect the observed data. Of these reactions, the reactivation of inactive empty I–E^k is negligible both because there is very little inactive I–E^k present due to the preloading and because the reactivation rate is very low ($t_{1/2} \geq 3$ h). The inactivation of active empty I–E^k is not very important at pH 5.3, as the $t_{1/2}$ of this reaction is 13 min, greater than four times the association duration. In contrast, at pH 7 the inactivation of active I–E^k may be much faster and could possibly greatly affect the experimental data (see Results). The dissociation of Ii–M complex to form M_a and free Ii peptide and the reassociation of this unlabeled peptide will both somewhat decrease the apparent association rate, as both reactions tend to decrease the length of time M_a is available to bind labeled peptide. However, simulations of the full reaction Scheme 4 show that most M_a is formed during the 5 min in which the Ii–M complex is incubated in the absence of peptide. They also show that the amount of free Ii peptide present is too low to compete very effectively for binding to M_a . Therefore, these side reactions do not greatly affect the observed data.

DISSOCIATION EXPERIMENTS

All dissociation experiments were performed at pH 5.3 and 37 °C in PBS-citrate. As in the association experiments, I–E^k pre-loaded with Ii 85–99 was incubated in the absence of added peptide for five minutes at pH 5.3 to generate a population of active empty MHC; 200 nM peptide was then added (for the PCC Q100Or mutants, 2 μM was used to obtain an adequate signal). The association reaction was allowed to proceed for either 3 min or overnight (approximately 20 h) before association was terminated and dissociation initiated by the addition of a >100-fold excess of unlabeled PCC Ac95–103 A103K. The dissociation reaction was monitored as previously described by periodically removing an aliquot from the reaction mixture, injecting it onto an HPSEC column to separate labeled peptide/I–E^k complex from free-labeled peptide, and measuring the

fluorescence intensity of the complex. For monophasic dissociation curves, rates of dissociation were determined by fitting to the data a curve of the following form: $C(t) = e^{-kt}$, where $C(t)$ is the amount of complex at time t divided by the amount at time 0 (immediately after the addition of unlabeled peptide) and k is the dissociation rate constant. For biphasic dissociation curves, the following equation was used: $C(t) = C_f e^{-k_f t} + C_s e^{-k_s t}$, where $C_f + C_s = 1$, C_f = the fractional magnitude of the fast phase, C_s = the fractional magnitude of the slow phase, k_f is the dissociation rate constant of the fast phase, and k_s is the dissociation rate constant of the slow phase.

RESULTS

Determination of the Rate of Peptide Association to I-E^k at pH 5.3. To determine the association rate of peptide to I-E^k, we measured peptide-MHC complex formation after adding variable concentrations of peptide to a fixed amount of active, empty I-E^k generated by the preloading scheme described previously (20). Observing peptide-dependence rather than time-dependence avoids a potential pitfall that has affected some previous experiments involving MHC; that is, when measuring the time-dependence of the binding of a fixed concentration of peptide, it is impossible to be certain that the rate-limiting step observed is actually the bimolecular association reaction and not a peptide-concentration-independent reaction of the MHC molecule.²

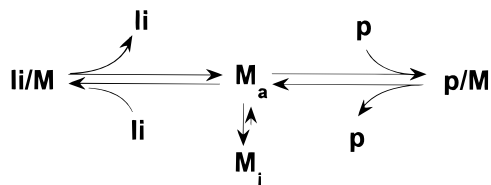
Association data for two peptides, Ii f85-99 and Ii f85-99 M90L, are shown in Figure 2. An approximate rate constant was calculated by fitting a single-exponential association curve to the data. Such a rate constant assumes a simplified reaction scheme (Scheme 3) for peptide binding to MHC:

Scheme 3



where M_a denotes MHC and the p denotes the labeled peptide. A more complete reaction scheme (Scheme 4) is as follows:

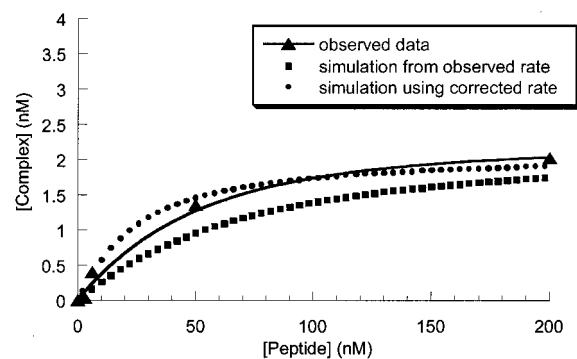
Scheme 4



where M_i is MHC that has been inactivated and Ii is an invariant chain peptide 85-99 (CLIP). Using this more complete reaction scheme, one can model peptide binding to I-E^k and calculate the rate constant that gives association behavior most consistent with the experimental data. Plotted in Figure 2 are: (a) the experimental data, (b) a single exponential fit to those data (implied by Scheme 3), (c)

² This problem may be circumvented by using low-peptide concentrations and short incubation durations. For example, we find that measurement of the association rate by adding 50 nM peptide to active MHC and varying the incubation time from 1 to 3 min yields similar association rates to those reported here.

(a) Ii f85-99



(b) Ii f85-99 M90L

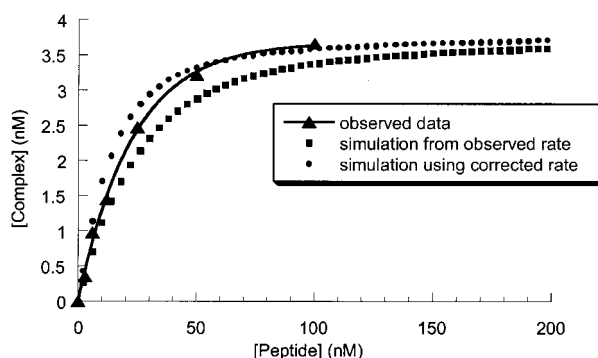


FIGURE 2: Determination of the association rate of peptide to active I-E^k at pH 5.3. Data shown indicate the amount of peptide-MHC complex produced after the reaction of I-E^k (8 nM) with varying concentrations of the indicated peptides for a fixed-length of time (3 min). The I-E^k used for the reaction was generated by allowing Ii 85-99/I-E^k complex to dissociate for 5 min in the absence of added peptide, resulting in approximately 55% active I-E^k. The association rate constant was estimated in two ways: (1) the experimental data were fit to a single-exponential equation describing a simplified situation, the reversible reaction of a fixed concentration of peptide with homogeneous, active, empty I-E^k, $[p/M] = [p]/([p] + K)[M_0](1 - e^{-(p+K)t})$ (fit represented by a solid line). Using this association rate, the full reaction scheme (Scheme 4) was simulated in Mathematica (data shown in small squares). (2) The full reaction scheme was simulated repeatedly in Mathematica to select the association rate constant resulting in simulated data most consistent with the experimental data (data shown in small circles).

simulated data obtained by plugging the association rate constant calculated above into the more complete Scheme 4, and (d) simulated data in which the association rate constant in Scheme 4 has been varied until the simulation was most consistent with experimental data (see Materials & Methods). For both peptides, rate constants obtained using Scheme 3 were slightly slower than the corrected rate constants obtained using Scheme 4—by a factor of 3.2 for Ii and a factor of 1.9 for Ii M90L. Simulations also predicted a somewhat greater amount of peptide-MHC complex than was observed experimentally. This may reflect errors in estimation of the amount of active MHC present or peptide-MHC complex formed. In addition, it is possible that reactions not included in Scheme 4, such as formation of short-lived peptide-MHC complex isomers, reduce the total amount of stable complex produced.

Association Rate Constants to I-E^k of 20 Peptides at pH 5.3. The experiments detailed in Figure 2 were performed for 20 different peptides with previously characterized

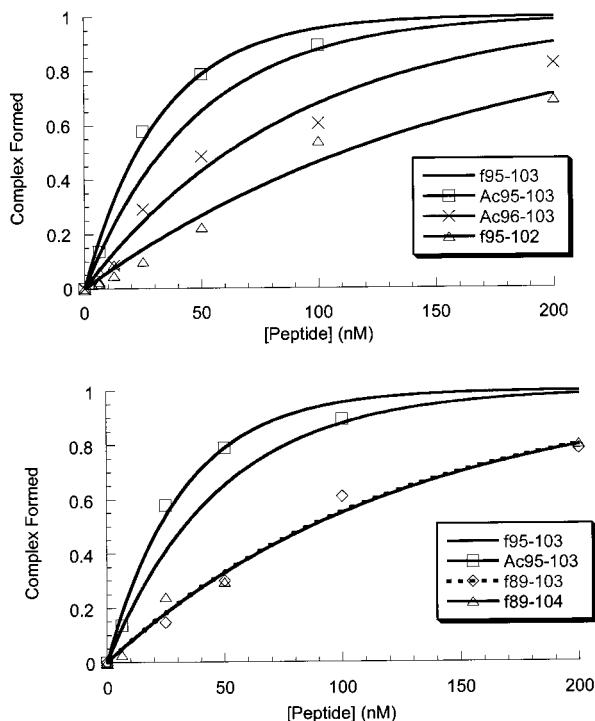


FIGURE 3: Effect of peptide elongation or truncation on association rate. (a) Truncation of the core-peptide sequence slows association. (b) Elongation of the core peptide sequence slows association. Peptide binding to active $I-E^k$ was measured as in Figure 2. The base peptide is PCC, and all of the peptides (except f95-102, which lacks position 103) have the mutation A103K, which naturally occurs in another commonly studied antigen, moth cytochrome *c*. This mutation is known to stabilize the binding of PCC to $I-E^k$. The curves shown are single-exponential fits to the data.

dissociation rates spanning a range of greater than 10000-fold. All peptides studied fit the general association profile shown in Figure 2, with binding well approximated by a single-exponential-curve fit. Rate constants and magnitudes of maximal binding estimated based in Scheme 3 are shown in Table 1. To obtain an estimate of the error involved in these association experiments, two independent measurements were performed for each of four peptides. The mean percent error was 13% for the association rate and 19% for the magnitude. On the basis of this error estimate, differences between rate constants of greater than 2-fold are unlikely to be due to chance alone ($p < 0.02$, assuming T distribution with four degrees of freedom).

One trend observed in the association rate constants reported is that peptides either shorter or longer than the nine amino acid core-binding sequence bind somewhat more slowly than the core sequence alone. Truncation of the core region of PCC 95-103 A103K (identical in sequence to moth cytochrome *c* 95-103) from nine amino acids to eight by deleting the p1 or p9 anchor residues resulted in a 2.5-fold decrease in the association rate constant (association plots shown in Figure 3a). These results indicate that efficient binding does not require initial contact at the p1 or the p9 anchor residue followed by association of the other residues in a directional fashion. The elongated peptides PCC f89-103 A103K and PCC f89-104 A103K, shown in Figure 3b, also had association rates slightly more than 3-fold slower than the core peptide PCC f95-103 A103K.

Two specially designed mutants of the PCC peptide were synthesized and studied in an attempt to test hypotheses

concerning the rate-limiting step in peptide binding to $I-E^k$. In one possible mechanism, the limiting factor in peptide-MHC association is the adoption of the extended polyproline peptide conformation observed in crystal structures of peptide bound to MHC (1-5). A mutant of PCC A103K (PCC-P) was, therefore, constructed in which four residues were mutated to prolines. These residues were chosen as ones in which single proline substitution had a minimal effect on complex stability (27). It was thought that the solution conformation of a peptide with such a large number of prolines would be more likely at any given time to resemble a type II polyproline helix. If the assumption of such a conformation were the limiting factor in binding to MHC, then such a peptide would have a faster association rate. The observed association rate of this peptide was in fact somewhat slower than, but comparable to, the nine amino acid PCC A103K peptide on which it is based. One possible explanation for a decreased association rate is cis-trans isomerization of the proline peptide bonds.

Another specially designed PCC A103K mutant was one in which four residues (the same four as in the proline mutant) were changed to glycines. If the assumption of a particular peptide backbone conformation is the limiting step in peptide-MHC association, the one would expect a glycine-substituted peptide to have a significantly different rate of association than the wild-type peptide, due to either increased conformational entropy or reduced side-chain steric clashes in some conformations. The experimentally determined association rate for the PCC-G was indeed lower than that of the unsubstituted peptide, but only by a factor of 2.8.

Dependence of Association Rate on Preloading Peptide. Association experiments for twelve of the peptides studied were carried out when the $I-E^k$ was preloaded with PCC Ac96-103 A103K and when it was preloaded with Ii 85-99. Binding data are shown in Table 2. The association rate measured with Ii preloading was correlated with that measured with PCC Ac96-103 A103K preloading. Within error, the calculated slope was 1 and the intercept 0 ($r^2 = 0.55$, $p < 0.01$). This suggests that the rate of peptide association to MHC does not depend on the peptide whose dissociation generates the active MHC.

Association of Peptides to $I-E^k$ at pH 7.0. The association behavior of 6 of the 20 peptides studied at pH 5.3 was also studied at pH 7. The dependence of complex formation on peptide concentration at pH 7 was, as at pH 5.3, well-approximated by a single-exponential association curve (Figure 4). Similar to previous reports, we also found that complex formation at pH 7 requires considerably higher concentrations of peptide than at pH 5.3—by an average factor of 130. Interestingly, the association curves of all six structurally varied peptides were similar, differing by no more than 13-fold in the peptide concentration required for half-maximal binding. Because of the uniformity of the change in association behavior between pH 5.3 and pH 7 for different peptides, it is unlikely that the pH-dependence reflects interactions between specific peptide side chains and the MHC protein.

We have previously shown that, similar to pH 5.3, the kinetics of peptide binding at pH 7 are consistent with reaction Scheme 4 (20). However, at pH 7, we cannot necessarily approximate Scheme 4 with Scheme 3, because this approximation assumes that the half-life of active $I-E^k$

Table 2: Kinetics of Peptide Binding are Highly Dependent on pH But Minimally Dependent on Peptide Structure or the Method Used to Generate Active I-E^a

| peptide | Ii 85–99 preloading at pH 5.3 | | PCC Ac96–103 A103K preloading at pH 5.3 | | Ii 85–99 preloading at pH 7.0 | |
|----------------------|--|-------------------|--|-------------------|---|-------------------|
| | rate (M ⁻¹ s ⁻¹) | magnitude (nM) | rate (M ⁻¹ s ⁻¹) | magnitude (nM) | rate ^b (M ⁻¹ s ⁻¹) | magnitude (nM) |
| Ii f85–99 M90L | 3.0 × 10 ⁵ | 3.6 | 2.6 × 10 ⁵ | 3.7 | 4.7 × 10 ³ | 3.5 |
| PCC f95–103 A103K | 3.0 × 10 ⁵ | 3.6 | 2.1 × 10 ⁵ | 2.8 | 9.5 × 10 ² | 2.1 |
| PCC Ac95–103fK A103K | 1.7 × 10 ⁵ | 2.0 | 2.5 × 10 ⁵ | 1.7 | | |
| PCC Ac96–103fK A103K | 6.9 × 10 ⁴ | 2.8 | 9.9 × 10 ⁴ | 2.5 | | |
| PCC Ac97–103fK A103K | 1.6 × 10 ⁵ | 1.6 | 1.1 × 10 ⁵ | 1.6 | | |
| PCC f95–102 | 3.7 × 10 ⁴ | 3.8 | 8.7 × 10 ⁴ | 2.4 | | |
| PCC f95–101 | 1.8 × 10 ⁵ | 2.5 | 6.0 × 10 ⁴ | 2.7 | | |
| PCC f89–103 | 4.0 × 10 ⁴ | 2.3 | 8.9 × 10 ⁴ | 1.5 | | |
| PCC f89–104 | 6.1 × 10 ⁴ | 3.3 | 7.4 × 10 ⁴ | 2.9 | 4.4 × 10 ² | 2.3 |
| PCC f89–103 A103K | 4.5 × 10 ⁴ | 3.5 | 8.1 × 10 ⁴ | 2.3 | 3.8 × 10 ² | ^c |
| PCC f89–104 Q100A | 4.5 × 10 ⁴ | 4.8 | 9.8 × 10 ⁴ | 3.1 | 7.9 × 10 ² | 2.3 |
| Hb | 2.0 × 10 ⁵ | 3.4 | 1.2 × 10 ⁵ | 4.0 | 8.3 × 10 ² | 3.0 |

^a Magnitudes and apparent association rates were determined from single-exponential binding curves as shown in Figures 2, 3, and 4 and described in the legend of Table 1. Active I-E^k was prepared by first preloading I-E^k with either Ii 85–99 or PCC Ac96–103 A103K at pH 5.3, 37 °C for five min. At this time, the indicated fluorescently labeled peptide was added for 3 min and its association measured. Data for Ii 85–99 preloading at pH 5.3 are a subset of the data shown in Table 1. Duplicate experiments were performed to measure the association rates to I-E^k preloaded with PCC Ac96–103 A103K for two peptides. The mean errors measured were 19% for the association rate and 15.5% for the maximal binding. Maximal errors were 32 and 23%, respectively. Similar experiments for one peptide with Ii preloading at pH 7.0 yielded errors of 12 and 6.6% for the apparent rate and maximal binding, respectively. Calculation of apparent association rates at pH 7 using eq 2 requires knowledge of the dissociation rates at pH 7. These rates were determined in a manner similar to that described for pH 5.3. ^b The apparent association rate at pH 7 may significantly underestimate the actual rate, because the half-life of the active isomer of empty I-E^k at pH 7 may be shorter than the 3 min duration of the association reaction (see text). ^c At pH 7, the magnitude for PCC f89–103 could not be calculated independently because saturation of binding occurred too slowly to be observed at experimentally feasible peptide concentrations, so the magnitude was constrained to that observed for PCC f95–103 A103K.

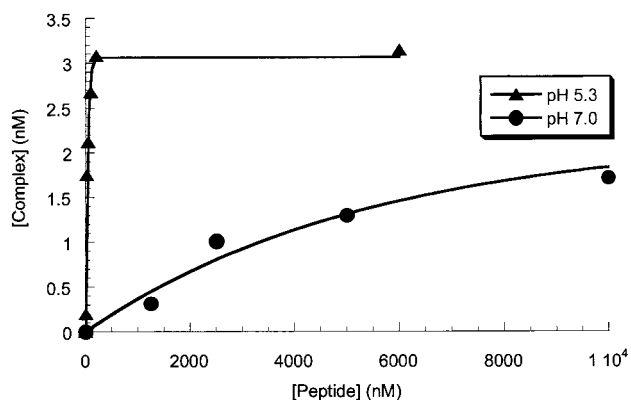


FIGURE 4: Effect of pH on peptide association to I-E^k. Association experiments were performed as previously described for PCC f95–103 A103K at pH 5.3 and pH 7.0. At neutral pH, approximately 100-fold more peptide was required to saturate binding than at mildly acidic pH. The curves shown are single-exponential fits used to determine the apparent association rate constants and magnitudes shown in Table 2.

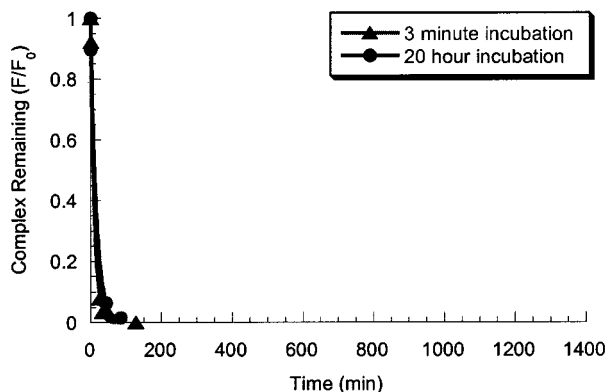
is greater than the duration of the association reaction (see Materials & Methods). The inactivation rate of active I-E^k at pH 7 has not yet been determined (preventing the simulation of Scheme 4 at pH 7). Preliminary experiments suggest that the inactivation rate at pH 7 is at least somewhat and potentially much faster than at pH 5.3 (J.R. and Judith Vacchino, unpublished data). Therefore, the approximately 100-fold decrease in the apparent association rates at pH 7 (see Table 2) relative to the association rates at pH 5.3 could be due either to a decrease in the second-order association rate constant or a decrease in the duration that the I-E^k is available to bind peptide (i.e., a decrease in the half-life of the active state).

Dissociation Behavior of Peptides Studied. The dissociation kinetics of many of the peptides studied in this report

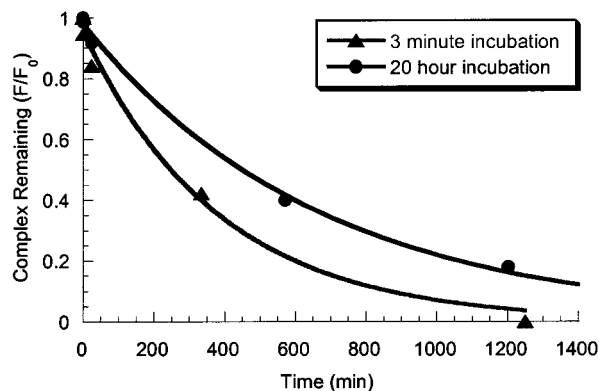
have been investigated previously, usually after association reactions of several hours. Since many peptides bind to class II MHC to form two or more isomeric complexes of differing stabilities, it was important to characterize the dissociation behavior of the peptides after both short (3 min) and long (overnight) incubation times. In this report, unlike most previous studies, we have terminated the binding reaction and initiated the dissociation measurement by adding a large excess of unlabeled peptide, without any intermediate purification step. Elimination of the purification step ensures that the dissociation behavior observed reflects the entire set of peptide–MHC complex isomers present at the end of the incubation period.

We find that 19 of the 20 peptides studied form one predominant kinetic complex, which is the same after either long or short association reactions. Specifically, 11 of the peptides form only short-lived complexes ($t_{1/2} < 2$ h, group A in Table 1, and exemplified in Figure 5A). Three of the peptides form mainly intermediate-lived complexes ($t_{1/2} = 2$ h to 1 day, group B in Table 1, and exemplified in Figure 5B). Five of the peptides form predominantly long-lived complexes ($t_{1/2} > 1$ day, group C in Table 1, and exemplified in Figure 5C). For peptides in groups A and B, the absence of long-lived isomeric complexes was determined by observing the dissociation of complexes formed after a long (overnight) association reaction until >95% of the signal was lost. In contrast to the apparent inability of the peptides in groups A or B to form any long-lived isomeric complexes, the peptides in both groups B and C tended to form some short-lived isomeric complexes. Our data are not well-suited to a precise characterization of the percentage of the short-lived isomeric complexes present for individual peptides. As expected, however, there was a trend toward the formation of a lower fraction of short-lived isomeric complexes with longer incubation duration, as exemplified in Figure 5B.

a. Ii f85-99 P95E



b. PCC f89-104



c. PCC f89-103 A103K

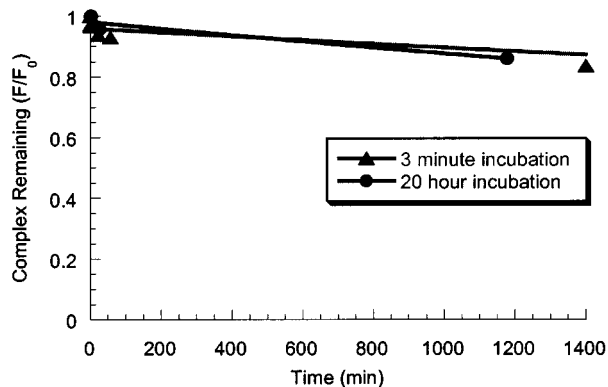


FIGURE 5: Characterization of the dissociation behavior of peptide–MHC complexes formed after short (3 min) and long (20 h) incubations. (a) Representative example of a peptide/I–E^k complex that exhibits a rapid, monophasic decay, even after a long incubation. (b) Representative example of a peptide/I–E^k complex that exhibits an intermediate decay after both short- and long-incubation periods. The curves shown represent single-exponential fits to the data. One can observe that a small fraction (<20%) of the complex dissociates much more rapidly. This fraction is somewhat greater after a short incubation period. (c) Representative example of a peptides/I–E^k complex that decays very slowly even after only a short-incubation period. As in (b), a small fraction (<20%) of the complex dissociates more rapidly. Amount of complex is measured relative to that present at time 0 in the dissociation.

Among the 19 peptides, which formed a predominant kinetic complex with I–E^k, several have particularly interesting dissociation kinetics. PCC–P is identical to the very stable binder PCC A103K, except for the substitution of four amino acid residues with proline. Although these residues

are not MHC contacts (p3, p5, p7, and p8), PCC–P dissociates very rapidly from I–E^k. This may reflect steric clashes caused by the large, rigid proline side chains. PCC–G, which has glycine in these four positions, also dissociates rapidly. This behavior suggests that the flexible glycine peptide bonds may increase the dissociation pathways available to the peptide. Finally, the unmutated PCC peptides are particularly interesting because previous work by Schmitt et al. has identified interconverting isomers of PCC bound to I–E^k at pH 7 by ¹⁹F NMR spectroscopy (16, 18). These isomers interconvert too rapidly to be kinetically distinguishable at pH 7, but lowering of the pH to 5.3 results in biphasic dissociation. As shown in Figure 5B, these peptides do form a substantial portion of short-lived isomeric complexes after a short association reaction at pH 5.3. However, the relationship between these complex isomers and those observed by Schmitt et al. after long association reactions remains unclear at this time.

PCC Q100Or: Association and Complex Isomers. In contrast to the 19 other peptides, one peptide did not form a predominant kinetic complex with I–E^k but instead appeared to form completely different complexes depending on the incubation duration. This peptide, PCC 89–104 Q100Or, dissociates in a monophasic fashion with a $t_{1/2}$ of 6 min after a short (3 min) incubation (Figure 6). However, when the same peptide is allowed to bind for 20 h, the dissociation behavior is biphasic. The fast phase, accounting for 73% of the initial signal, has a $t_{1/2}$ of approximately 6 min, while the slow phase has a $t_{1/2}$ of greater than 100 hours. This finding shows that one or more long-lived isomers of the Q100Or complex exist and have formation time substantially longer than the short-lived isomer(s). A long incubation causes a progressive accumulation of these long-lived complexes. To investigate further the binding of PCC 89–104 Q100Or to I–E^k, we synthesized a shorter peptide consisting of only the putative core-binding sequence, PCC 95–103 Q100Or. After a short incubation period, the complexes formed between this peptide and I–E^k were too unstable ($t_{1/2} < 1$ min) for their association or dissociation rates to be accurately quantitated using our methods. However, after an overnight incubation in the presence of large (5 μ M) concentrations of peptide, approximately 50% of the complexes formed were very stable ($t_{1/2} > 24$ h). These findings suggest that the readily detectable short-lived complexes with $t_{1/2}$ of 6 min formed between PCC 89–104 Q100Or and I–E^k require PCC residues 89–94 and/or 104. The ability of the short PCC 95–103 Q100Or peptide to form slowly a stable complex with I–E^k, however, suggests that the stable isomer between the longer peptide and I–E^k indeed utilizes the core registry of wild-type PCC (residue 95 in the p1 pocket).

DISCUSSION

In this report, we characterize the kinetics of twenty different peptides binding to the class II MHC protein I–E^k. All twenty peptides bind with similar association rate constants, despite having dissociation rate constants that span a range of greater than 10000-fold. A previously reported example of a peptide–protein association reaction in which the mutation of peptide side chains greatly affects complex affinity without substantially affecting k_{on} is that between two fragments of ribonuclease A to form a complex

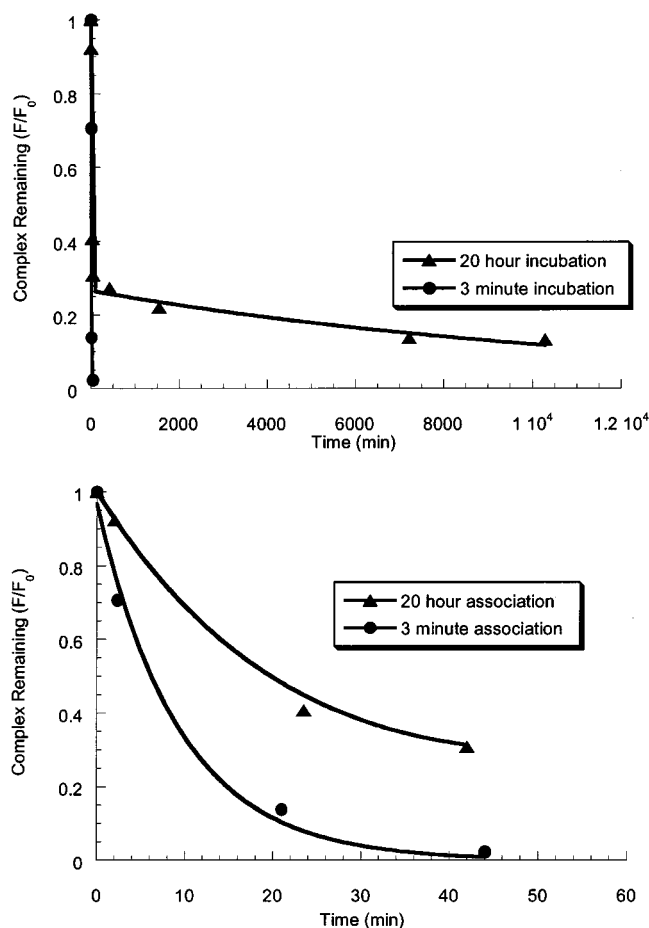


FIGURE 6: Dissociation of I-E^k/PCC f89-104 Q100Or complex. (a) After a short (3 min) incubation period, all of peptide/I-E^k complex formed is unstable, with a $t_{1/2}$ of 6 min. After a longer (20 h) incubation, 73% of the complex formed is unstable ($t_{1/2} \approx 6$ min), while the remaining 27% of the complex is very stable, with a $t_{1/2}$ of greater than 100 hours. The curves shown represent a monoexponential fit for the 3 min data and a biexponential fit for the 20 h data. (b) Shows an enlargement of the first hour of dissociation. Amount of complex is measured relative to that present at time 0 in the dissociation.

corresponding to the full enzyme (28). Independent or concerted mutations at two sites on the smaller, 20 amino acid fragment result in an increase in k_{off} by up to 6 orders of magnitude, but only a 3-fold decrease in k_{on} . From these results, Goldberg and Baldwin conclude that the transition state for the association-dissociation reaction must not depend greatly on interactions between the protein and side chains of the peptide, but likely on nonspecific hydrophobic ones. We similarly conclude that the transition state for peptide-MHC complex association-dissociation does not depend greatly on interactions between the protein and side chains of the peptide. However, because peptide-MHC complexes are stabilized by 11-17 hydrogen bonds between the MHC protein and the peptide backbone, we hypothesize that the transition state for peptide binding may involve the formation of some of these bonds.

A difference between peptide-MHC association and the ribonuclease A system is that the ability of ribonuclease A to bind mutated peptides with a relatively constant association rate is not directly related to the enzyme's function. MHC molecules, on the other hand, must be able to bind a wide variety of peptides and present them for immune recognition.

MHC molecules traverse the endosomal pathway from assembly to peptide presentation on the cell surface in approximately 30 min (29). The interval during which they are available for peptide binding is thus fairly short when compared to the previously observed time-scales of peptide association and dissociation (7, 11, 27). Many immunogenic peptides form complexes with MHC that are stable for hours (sometimes even in the presence of HLA-DM, the peptide exchange catalysts present in endosomes) (24, 25). Therefore, when multiple such peptides are present in the endosomes, the association reaction between the different peptides and MHC does not reach equilibrium. If association rates varied widely between peptides, then one could envision a fast-binding peptide that would bind to all the available MHC and screen out others from immune surveillance. Consistent with the function of MHC being the presentation of a wide variety of peptides, we found that most of the peptides we studied bind with a rate constant of approximately $10^5 \text{ M}^{-1} \text{ s}^{-1}$ at mildly acidic pH, with no peptide binding with a rate constant greater than $5 \times 10^5 \text{ M}^{-1} \text{ s}^{-1}$.

An interesting feature of peptide binding to MHC is that a single peptide can bind to a single MHC protein to form multiple isomeric peptide-MHC complexes of differing stability. Experiments using peptide mutations, T cell recognition, and ¹⁹F NMR spectroscopy suggest that these isomers can result from both the peptide binding in different backbone registries and differences in complex conformation with the peptide bound in a single registry (16, 19, 30, 31). Interestingly, we find that 19 of the 20 peptides studied tend to dissociate with similar kinetics after either very short (<3 min) or longer (overnight) incubations. This shows that even after only three minutes, the set of peptide-MHC complex isomers present usually resembles the equilibrium set of isomers.

Such a rapid formation of a specific peptide-MHC complex isomer could occur in several ways. Free-energy diagrams for three such possibilities are shown in Figure 7. In the first model (Figure 7A), ΔG^\ddagger for one particular registry is much lower than for the others. That registry would then have a much faster k_{on} and be kinetically favored. Our experimental data, however, suggest that this model is unlikely to be accurate. The truncation studies that we report here indicate that a slight backbone elongation or truncation in a given direction is unlikely to have a large (greater than 10-fold) effect on binding kinetics. Our experiments testing the effects of many mutations suggest that k_{on} , and thus ΔG^\ddagger , is largely independent of peptide side-chain structure.

Another possibility (Figure 7B) is that the peptide, once loosely bound, can arrange itself on the MHC protein in the most energetically favorable registry. Experiments designed to test this hypothesis and performed in our laboratory find no evidence for such behavior in the I-E^k system (Michael Belmares and H. M. M., unpublished data).

In the third model (Figure 7C), different registries bind to the MHC with distinct transition states that nevertheless have similar ΔG^\ddagger 's for binding. These registries, however, have substantially different energies when bound to MHC. The resulting disparity among off-rates provides a means of registry selection. Since for all but one peptide a single predominant kinetic complex is detected after a three-minute incubation period, the registries that are not observed (or constitute a small minority of the complexes detected) likely

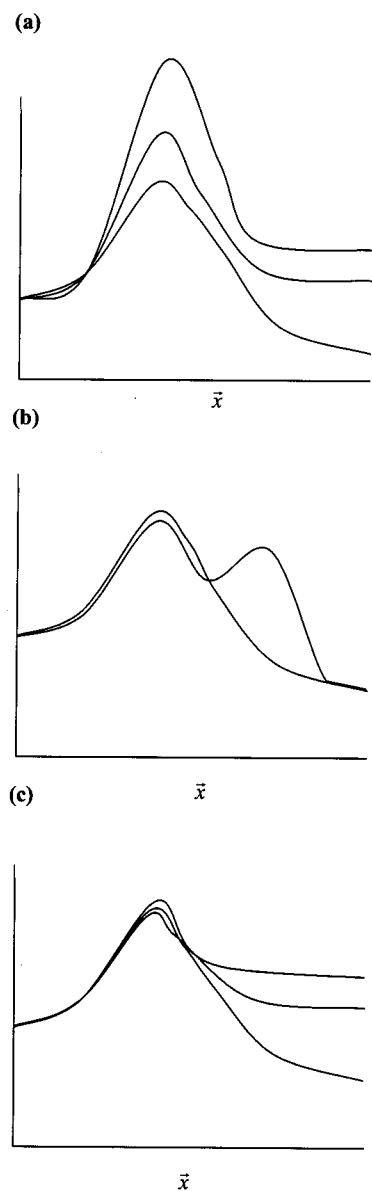


FIGURE 7: Model free-energy diagrams for peptide-MHC association. The graphs represent schematic plots of free-energy vs arbitrary reaction coordinate. Model (a): Different registries (A, B, and C) have different ΔG^\ddagger 's for association to MHC. Model (b): After loosely associating in one registry, a peptide can shift to a more stable registry, while remaining bound to the MHC. Model (c): Different registries have distinct transition states for binding to MHC but similar ΔG^\ddagger 's.

have dissociation half-times considerably faster than three minutes.

The one peptide (PCC 89–104 Q100Or) that rapidly forms an unstable complex but only slowly forms a stable complex demonstrates that a higher energy barrier can limit the formation of a certain peptide-MHC complex isomer. It is not known whether the stable complex utilizes the same registry as the rapidly formed but unstable one or whether the unstable isomer can convert to the stable one without dissociation.

With the possible exception of the above case, the transition state model schematized in Figure 7C provides an explanation for registry selection that is consistent with the experimental data. It is also consistent with our finding that peptides longer than the nine amino acid core tend to bind

more slowly than peptides limited to the core amino acids, as longer peptides bind in a greater number of unstable registries. However, since there are only on the order of 10 potential registries per peptide, this model alone is not sufficient to explain why the rate of peptide association to MHC is 4 orders of magnitude slower than the Smoluchowski diffusion limit.

We, therefore, propose that the allowable peptide conformations for binding are relatively few, so only a small proportion of the collisions between peptide and MHC result in binding events. This picture is consistent with the previously reported binding kinetics of the peptide charybotoxin to Ca^{2+} -activated K^+ channels at high-salt concentrations (32). In that instance, association was diffusion-limited, yet slow (rate constants of $\sim 10^5 \text{ M}^{-1} \text{ s}^{-1}$). Peptide-MHC complex formation is likely the result of relatively rare collisions between peptide and MHC. Most such collisions produce very unstable complexes (dissociation $t_{1/2} < 10 \text{ s}$), rapidly releasing the peptide and empty MHC protein to repeat the binding process. Only a few of these binding events result in transition states involving the peptide bound in the most favorable registry.

ACKNOWLEDGMENT

Johannes Kratz provided the Hb 64–76 peptide as well as data on the dissociation of Hb from I-E^k. Michael Liang provided several of the Ii mutant peptides. We would also like to thank Tom Andersen for critical reading of the manuscript and Marija Vrljic, Judith Vacchino, and Michael Belmares for many helpful discussions.

REFERENCES

1. Stern, L. J., Brown, J. H., Jardetzky, T. S., Gorga, J. C., Urban, R. G., Strominger, J. L., and Wiley, D. C. (1994) *Nature* 368, 215–21.
2. Ghosh, P., Amaya, M., Mellins, E., and Wiley, D. C. (1995) *Nature* 378, 457–62.
3. Dessen, A., Lawrence, C. M., Cupo, S., Zaller, D. M., and Wiley, D. C. (1997) *Immunity* 7, 473–81.
4. Murthy, V. L., and Stern, L. J. (1997) *Structure* 5, 1385–96.
5. Fremont, D. H., Hendrickson, W. A., Marrack, P., and Kappler, J. (1996) *Science* 272, 1001–4.
6. Roof, R. W., Luescher, I. F., and Unanue, E. R. (1990) *Proc. Natl. Acad. Sci. U.S.A.* 87, 1735–9.
7. Roche, P. A., and Cresswell, P. (1990) *J. Immunol.* 144, 1849–56.
8. Reay, P. A., Wettstein, D. A., and Davis, M. M. (1992) *EMBO J.* 11, 2829–39.
9. Witt, S. N., and McConnell, H. M. (1991) *Proc. Natl. Acad. Sci. U.S.A.* 88, 8164–8.
10. Sadegh-Nasseri, S., and McConnell, H. M. (1989) *Nature*. 337, 274–6.
11. Witt, S. N., and McConnell, H. M. (1994) *Biochemistry* 33, 1861–8.
12. Sadegh-Nasseri, S., Stern, L. J., Wiley, D. C., and Germain, R. N. (1994) *Nature* 370, 647–50.
13. Mason, K., Denney, D. W. Jr., and McConnell, H. M. (1995) *J. Immunol.* 154, 5216–27.
14. Mason, K., and McConnell, H. M. (1994) *Proc. Natl. Acad. Sci. U.S.A.* 91, 12463–6.
15. Beeson, C., and McConnell, H. M. (1994) *Proc. Natl. Acad. Sci. U.S.A.* 91, 8842–5.
16. Schmitt, L., Boniface, J. J., Davis, M. M., and McConnell, H. M. (1998) *Biochemistry* 37, 17371–80.

17. Viner, N. J., Nelson, C. A., Deck, B., and Unanue, E. R. (1996) *J. Immunol.* 156, 2365–8.
18. Schmitt, L., Boniface, J. J., Davis, M. M., and McConnell, H. M. (1999) *J. Mol. Biol.* 286, 207–18.
19. Rabinowitz, J. D., Tate, K., Lee, C., Beeson, C., and McConnell, H. M. (1997) *Proc. Natl. Acad. Sci. U.S.A.* 94, 8702–7.
20. Rabinowitz, J. D., Vrljic, M., Kasson, P. M., Liang, M. N., Busch, R., Boniface, J. J., Davis, M. M., and McConnell, H. M. (1998) *Immunity* 9, 699–709.
21. Natarajan, S. K., Assadi, M., and Sadegh-Nasseri, S. (1999) *J. Immunol.* 162, 4030–4036.
22. Springer, S., Doring, K., Skipper, J. C., Townsend, A. R., and Cerundolo, V. (1998) *Biochemistry* 37, 3001–12.
23. Pieters, J. (1997) *Curr. Opin. Immunol.* 9, 89–96.
24. Weber, D., Evavold, B., and Jensen, P. (1996) *Science* 274, 618–20.
25. Sloan, V. S., Cameron, P., Porter, G., Gammon, M., Amaya, M., Mellins, E., and Zaller, D. M. (1995) *Nature* 375, 802–6.
26. Wettstein, D. A., Boniface, J. J., Reay, P. A., Schild, H., and Davis, M. M. (1991) *J. Exp. Med.* 174, 219–28.
27. Reay, P. A., Kantor, R. M., and Davis, M. M. (1994) *J. Immunol.* 152, 3946–57.
28. Goldberg, J. M., and Baldwin, R. L. (1998) *Biochemistry* 37, 2556–63.
29. Marsh, E. W., Dalke, D. P., and Pierce, S. K. (1992) *J. Exp. Med.* 157, 425–436.
30. Rotzschke, O., Falk, K., Mack, J., Lau, J. M., Jung, G., and Strominger, J. L. (1999) *Proc. Natl. Acad. Sci. U.S.A.* 96, 7445–50.
31. Quaratino, S., Thorpe, C. J., Travers, P. J., and Londei, M. (1995) *Proc. Natl. Acad. Sci. U.S.A.* 92, 10398–402.
32. Miller, C. (1990) *Biochemistry* 29, 5320–5325.
33. Schwartz, R. H., Fox, B. S., Fraga, E., Chen, C., and Singh, B. (1985) *J. Immunol.* 135, 2598–608.
34. Evavold, B. D., Williams, S. G., Hsu, B. L., Buus, S., and Allen, P. M. (1992) *J. Immunol.* 148, 347–53.
35. Schild, H., Gruneberg, U., Pougialis, G., Wallny, H. J., Keilholz, W., Stevanovic, S., and Rammensee, H. G. (1995) *Int. Immunol.* 7, 1957–65.

BI9921337